Contribution from the Department of Chemistry,
Purdue University, West Lafayette, Indiana 47907

Photochemistry of Copper(III) Complexes of Peptides with α-Aminoisobutyric Acid Residues

ARLENE W. HAMBURG and DALE W. MARGERUM*

Received March 8, 1983

Replacement of α-carbon hydrogens by methyl groups in the amino acid residues of peptide complexes of copper(III) decreases the rate of thermal decomposition but enhances photochemical decomposition. Copper(III)–peptide disappearance quantum yields are wavelength dependent with different plateau values for the two ligand-to-metal charge-transfer (LMCT) transitions. The plateau quantum yields range from 0.1 to 0.5 and depend on the structure of the ligand. Suggested primary photoproducts from irradiation of the two LMCT bands are copper(II)-coordinated σ and π amidyl radicals. The final products of the photodecomposition are copper(II) and peptide fragments that result from C–C bond cleavage in the first, second, or third residue of the peptide ligand radical. The amount and identity of the products depend on the LMCT band irradiated as well as the pH, which affects the extent of coordination of the amidyl radical by copper(II) during fragmentation. The effect of ligand structure on metal–peptide photoactivity is examined by variation of the identity of the amino acid residues and the peptide length.

Introduction

Peptide complexes of copper(III) exhibit variable stability toward redox decomposition with lifetimes of seconds to weeks in aqueous solution[1-6] for peptides containing α-carbon hydrogens. In contrast, Aib_3, the tripeptide of α-aminoisobutyric acid, which has no α-carbon hydrogens, forms a copper(III) complex that is stable to thermal intramolecular redox decomposition over periods of many months in neutral or acidic solutions.[3] A crystal structure[7] of the $Cu^{III}(H_{-2}Aib_3)$ complex (**1**) shows the copper to be four-coordinate with a nearly

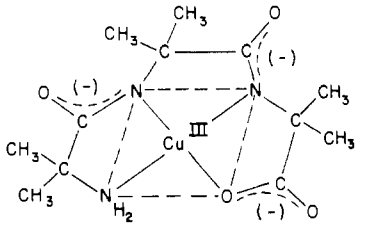

1

square-planar geometry and with short (1.80 Å) copper–N(peptide) bonds. In contrast to its thermal stability, this complex is very sensitive to photochemical decomposition by ultraviolet and visible radiation. The photoreaction is ligand oxidation and metal reduction as opposed to aquation or solvent oxidation. Earlier work[3] showed that after complete photolysis approximately 50% of Aib_3 is recovered along with a 50% yield of acetone and carbon dioxide (relative to the initial $Cu^{III}(H_{-2}Aib_3)$ concentration). Quantum yields for photodecomposition of other copper(III) complexes were determined previously to be 0.06 at 366 nm[4] for the tetraglycine complex, $Cu^{III}(H_{-3}G_4)^-$, and 0.008 at 278 nm[6] for a macrocyclic peptide complex, $Cu^{III}(H_{-4}C)^-$, where C is *cyclo*-(β-alanylglycyl-β-alanylglycyl).[8] The present work shows that the quantum yields for **1** are much higher with values of 0.34 at 278 nm and 0.23 at 366 nm.

Two intense absorption bands are seen in the ultraviolet–visible spectra of copper(III)–peptide complexes, one at 250–280 nm and the other at 360–400 nm. The high oxidation state of copper and the large molar absorptivities ($\epsilon \simeq 5000$–$11\,000$ M^{-1} cm^{-1}) of the bands indicate that they are ligand-to-metal charge-transfer (LMCT) transitions. Comparison of the absorption spectra for various copper(III)–peptide complexes leads to the assignment of the high-energy band as a σ-LMCT transition and the low-energy band as a π-LMCT transition. Similar assignments of σ-LMCT and π-LMCT have been made for the CT bands in the spectra of halide complexes of other d^8, square-planar transition metals, gold(III), platinum(II), and palladium(II).[9]

In the present work the quantum yield and photodecomposition stoichiometry of **1** is reported as a function of the wavelength of irradiation and medium conditions. The disappearance quantum yield varies greatly with wavelength but exhibits plateau regions for irradiation within each LMCT band. Also, a different product stoichiometry is seen for each LMCT band. Variations in solution pH do not affect the quantum yields but do change the identity of the photodecomposition products. On the basis of wavelength dependence of the quantum yield and photodecomposition stoichiometry as well as the pH dependence of product identity, a mechanism is proposed that involves the formation and fragmentation of σ and π copper(II)–amidyl radicals. The photochemical behavior of other copper(III)–peptide complexes shows that the quantum yield and the product stoichiometry are dependent on the peptide length and the number of α-carbon methyl substitutents.

Experimental Section

Reagents. Copper(II) perchlorate solution, prepared from $CuCO_3$ and $HClO_4$, was standarized by EDTA titration. Copper(III)–peptide solutions were prepared by electrochemical oxidation of the corresponding copper(II)–peptide solutions.[10] The peptide ligands were synthesized by the dicyclohexylcarbodiimide method of amino acid coupling.[3] Liquid chromatographic solvents were distilled-in-glass grade, and other organic solvents were spectrophotometric grade. The

(1) Margerum, D. W.; Chellappa, K. L.; Bossu, F. P.; Burce, G. L. *J. Am. Chem. Soc.* **1975**, *97*, 6894.
(2) Burce, G. L.; Paniago, E. B.; Margerum, D. W. *J. Chem. Soc., Chem. Commun.* **1975**, 261.
(3) Kirksey, S. T., Jr.; Neubecker, T. A.; Margerum, D. W. *J. Am. Chem. Soc.* **1979**, *101*, 1631.
(4) Rybka, J. S.; Kurtz, J. L.; Neubecker, T. A.; Margerum, D. W. *Inorg. Chem.* **1980**, *19*, 2791.
(5) Bossu, F. P.; Chellappa, K. L.; Margerum, D. W. *J. Am. Chem. Soc.* **1977**, *99*, 2195.
(6) Rybka, J. S.; Margerum, D. W. *Inorg. Chem.* **1981**, *20*, 1453.
(7) Diaddario, L. L.; Robinson, W. R.; Margerum, D. W. *Inorg. Chem.* **1983**, *22*, 1021.
(8) Abbreviations for the amino acid residues in peptides are as follows: G, glycyl; A, α-alanyl; β-A, β-alanyl; Aib, α-aminoisobutyryl; C, *c*-(β-AGβ-AG); a, amide; *N*-f, *N*-formylamine; H_{-n} refers to *n* deprotonated peptide nitrogens coordinated to copper.
(9) Gray, H. B. *Transition Met. Chem.* (*N.Y.*) **1965**, *1*, 239.
(10) Neubecker, T. A.; Kirksey, S. T., Jr.; Chellappa, K. L.; Margerum, D. W. *Inorg. Chem.* **1979**, *18*, 444.

0020-1669/83/1322-3884$01.50/0

spin-trap reagents, 5,5-dimethyl-1-pyrroline *N*-oxide, DMPO, and *N*-*tert*-butyl-α-phenylnitrone, PBN, were purchased from Aldrich. DMPO was purified before use to remove radical impurities.[11]

Instrumentation. Continuous Photolysis. The optical train for continuous photolysis consisted of the lamp housing (Oriel 6141) fitted with a 1000-W HgXe arc lamp (Hanovia 977-B1), collimating lenses, a 100-mm path length water filter (Oriel 6214), a focusing lens, monochromator (Oriel 7240), appropriate filters, and the sample cell. The arc lamp was powered by an Oriel Universal power supply (Model 8540). The band-pass of the monochromator was ~6 nm with 1-mm slits with gratings blazed at either 280 or 500 nm. Ultraviolet grade optics were used throughout. The sample cell was a thermostated 1-cm rectangular cuvette holder (Varian) mounted above a magnetic stirring motor (Tri-R Instruments, Model MS-7).

Reversed-Phase Liquid Chromatography (RPLC). The liquid chromatograph was a Waters 6000A solvent delivery system equipped with a Waters U6K injector. The detector was a modified Beckman DU spectrophotometer. The monitoring wavelength was 206 nm. Either an Altex Ultrasphere-IP C18 5-μm column or a Waters RCM-100 radial-compression unit equipped with a Waters Radial-PAK C18 5-μm cartridge was used for separation of the peptide products from the photodecomposition.

Other Instrumentation. Fluorescence spectra were recorded on a Perkin-Elmer spectrophotometer, Model MPF-44B. Ultraviolet–visible absorption spectra were recorded on either a Cary 14, Hewlett-Packard 8450A, or a Perkin-Elmer 320 spectrophotometer. EPR spectra were measured at −150 °C by using a Varian E-109 X-band EPR modulated at 100 kHz with a Varian E-935 data acquisition system. ^{1}H NMR spectra were obtained on a Varian XL-200 instrument.

Methods. Argon-saturated solutions were photolyzed at 25 °C. Light intensity, I_0, was determined by ferrioxalate actinometry.[12] To evaluate the quantum yield for loss of copper(III), ϕ, the left-hand side (LHS) of eq 1 was plotted vs. the irradiation time, t. The loss

$$\frac{\Delta[\mathrm{Cu(III)}]}{I_0(\mathrm{Fr})} = \phi t \qquad (1)$$

of copper(III) was monitored spectrophotometrically. The fraction of light absorbed, Fr, is equal to $1-10^{-A}$ where A is the absorbance at the wavelength of irradiation. Generally, optically opaque solutions ($A.> 3$) were irradiated so that Fr = 1. At longer wavelengths it was not always possible to prepare solutions with $A > 3$. In these cases, eq 2 was used to evaluate ϕ, where ϵ is the molar absorptivity

$$\frac{1}{I_0}\left(\Delta[\mathrm{Cu(III)}] + \frac{1}{2.3\epsilon b}\log\frac{\mathrm{Fr}_0}{\mathrm{Fr}_t}\right) = \phi t \qquad (2)$$

of the copper(III) complex at the wavelength of irradiation and Fr_0 and Fr_t are the fractions of light absorbed by the solution before and after photolysis, respectively. For those wavelengths where the copper(II)–peptide complexes (formed from the photolysis of the copper(III) complexes) did not absorb, plots of the LHS of eq 1 or 2 vs. t were linear with a zero intercept. For irradiation at λ <278 nm, the products of the photodecomposition absorb. At these wavelengths the absorbance vs. time data were treated by an extension of the method purposed by Bunce[13] (eq 3), where A_0 is the absorbance

$$\frac{1}{I_0}\Bigg(\Delta[\mathrm{Cu(III)}] \times \left(1 - \frac{\epsilon^{\mathrm{P}}}{\epsilon^{\mathrm{Cu}}}\right) + \frac{A_0 + \epsilon^{\mathrm{P}}[\mathrm{Cu(III)}]_0}{\epsilon^{\mathrm{Cu}}}\ln\frac{[\mathrm{Cu(III)}]_0}{[\mathrm{Cu(III)}]_t}\Bigg) = \phi t \qquad (3)$$

of any copper(II) complex present initially due to incomplete oxidation to copper(III) and ϵ^{P} and ϵ^{Cu} are the molar absorptivities of the products and the copper(III) complex, respectively, at the wavelength of irradiation. Molar absorptivities of the copper(III)–peptide complexes were determined by ascorbic acid titration.

The amino acid, amino acid amide, and peptide products of the photodecomposition were determined by reversed-phase liquid chromatography. Calibration curves, prepared from authentic compounds, used peak height measurements for quantitation. The mobile phase was either 0.1 M phosphate buffer for the Altex column or 0.1 M phosphate buffer/0.2 M $NaClO_4$ for the Waters cartridge. The pH of the mobile phase was 2.2 for separation of the amino acid and the amino acid amides from the solvent front and 5.4 for separation of the longer peptide fragments. The peptide fragments were identified by matching retention times in at least two different mobile phases.

The RPLC retention time of one major fragment observed in photolysis mixtures at pH 9 could not be matched to any presently available peptide containing the Aib residue. Its retention time as a function of pH and its extraction behavior indicated that an acidic functional group was present. The fragment was isolated through a series of extractions followed by RPLC separation and evaporation of the solvent. The resulting residue was dissolved in D_2O or acetone-d_6 for NMR data and was dissolved in chloroform for IR data. The residue was analyzed by both CI and EI mass spectrometry using a Finnigan 4000 instrument with an ionizing energy of 70 eV and a source temperature of 250 °C. Fragmentation of the residue by electron impact gave a characteristic loss of CO_2H for an acid and gave a $^+C(CH_3)_2NCO$ fragment and other fragments typical of hydantoins.[14] The parent masses by both CI and EI mass spectrometry confirmed the assignment of the residue as the 3-substituted hydantoin (**2**). The NMR and IR data were consistent with this assignment.

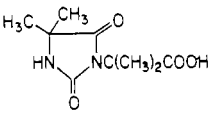

2

Results and Discussion

Copper(III)–Peptide Electronic Absorption Spectra. The ultraviolet–visible absorption data for several classes of copper(III)–peptide complexes are given in Table I. Suggested structures for the complexes in solution are **3** and **4**, where

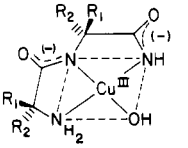

3, $Cu^{III}(H_{-2}L_2a)(OH)$

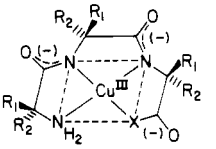

4a, X = O, $Cu^{III}(H_{-2}L_3)$
b, X = NH, $Cu^{III}(H_{-3}L_3a)$
c, X = $NCR_1R_2CO_2^-$, $Cu^{III}(H_{-3}L_4)^-$

for Aib, $R_1 = R_2 = CH_3$, for A, R_1 = H and $R_2 = CH_3$, and for G, $R_1 = R_2$ = H. The UV–vis spectra of all copper(III)–peptide complexes presently examined have at least two intense absorption bands in the region 40 000–25 000 cm^{-1} (250–500 nm). The energy separation between the two bands, ΔE, varies between (10.4–12.6) × 10^3 cm^{-1} and is dependent upon the number of α-carbon methyl groups in the ligand. The intensity of the two absorption features and the high oxidation state of copper indicate that the transitions are ligand-to-metal charge-transfer (LMCT) bands.[15] Ligand field (LF) transitions are seen only for the tetrapeptide ligands. Presumably,

(11) Ahn, B.-T.; McMillin, D. R. *Inorg. Chem.* **1981**, *20*, 1427.
(12) Calvert, J. G.; Pitts, J. N., Jr. "Photochemistry"; Wiley: New York, 1966; pp 783–785.
(13) Bunce, N. F. *J. Photochem.* **1981**, *15*, 1.
(14) Corral, R. A.; Orazi, O. O.; Duffield, A. M.; Djerassi, C. *Org. Mass Spectrom.* **1971**, *5*, 551.
(15) Jørgensen, C. K. *Prog. Inorg. Chem.* **1970**, *12*, 101.

Table I. Ultraviolet-Visible Spectral Data for Copper(III)-Peptide Complexes

peptide[a]	λ_{max}, nm (ϵ, M^{-1} cm^{-1})	$10^{-3}\Delta E$, cm^{-1} [b]	donor atoms[c]
dipeptide amide			
Aib_2a	275, 385	10.4	N_a, 2 N_p, O_h
tripeptides			
Aib_3	278 (11 500), 395 (5200 ± 40)	10.7	N_a, 2 N_p, O_c
$AAib_2$	278 (11 200), 391 (5200 ± 40)	10.4	N_a, 2 N_p, O_c
A_3[d]	270, 385	11.0	N_a, 2 N_p, O_c
GAG[e]	267, 385	11.5	N_a, 2 N_p, O_c
tripeptide amide			
Aib_3a	260 (10 500), 364 (6870 ± 90)	11.0	N_a, 3 N_p
tetrapeptides			
Aib_3G[f]	265 (10 170), 373 (7260 ± 40), ~550 (300)	10.9	N_a, 3 N_p
G_2AibG	255 (10 000), 365 (8270 ± 30), ~550 (320)	11.8	N_a, 3 N_p
A_3G[e]	257, 362	11.3	N_a, 3 N_p
G_4[g]	250, 365, ~550	12.6	N_a, 3 N_p
cyclic peptide			
c-(β-AG-β-AG)[h]	250 (12 000), 365 (6200), 275 (10 500) sh	12.6	4 N_p
N-formyl peptides[i]			
N-fG_4	~250, 357	~12.0	4 N_p
N-fG_3a	~250, 345	~11.0	4 N_p
N-fG_3	~250, 365	~12.6	3 N_p, O_c
Aib_3 (nonaqueous solvents)			
2-propanol	278 (10 700), 408 (5700)	11.5	N_a, 2 N_p, O_c
CH_3CN	276 (9700), 416 (5700)	12.2	N_a, 2 N_p, O_c
Me_2SO	276 (9800), 414 (5900)	12.0	N_a, 2 N_p, O_c
pyridine	*j*, 418 (6100)		N_a, 2 N_p, O_c

[a] Aqueous medium unless otherwise noted; 0.1 M acetate, pH 5.0, μ = 0.1 M ($NaClO_4$) for all Aib-containing ligands. [b] Energy separation between the two LMCT bands. [c] Abbreviations used are as follows: N_a, amine nitrogen; N_p, deprotonated peptide amide nitrogen; O_c, carboxylate oxygen; O_h, hydroxide oxygen. [d] Farkas, J. M. M.S. Thesis, Purdue University, 1982. [e] Read, R. A. Ph.D. Thesis, Purdue University, 1982. [f] Axup, A.; Hinton, J. P.; Margerum, D. W., unpublished data. [g] Reference 4. [h] Reference 6. [i] Reference 10. [j] Masked by pyridine absorption.

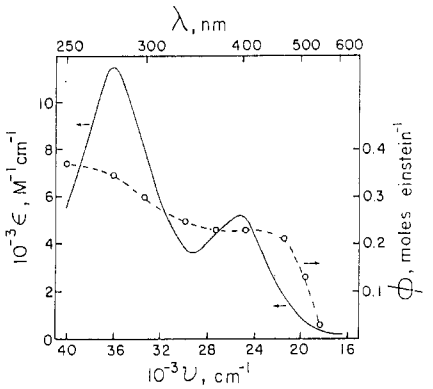

Figure 1. Disappearance quantum yield wavelength dependence and ultraviolet-visible absorption spectrum for $Cu^{III}(H_{-2}Aib_3)$ (0.1 M acetate, pH 5.0, μ = 0.1 M ($NaClO_4$)): ϕ, ---; UV-vis spectrum, — (ϵ = molar absorptivity).

the LF transitions for the copper(III) complexes of the other peptide ligands are masked by their charge-transfer absorption bands.

The LMCT transitions could originate from molecular orbitals localized on either carboxylate (or hydroxide) oxygen, amine nitrogen, or deprotonated peptide nitrogen. For example, the transient species $Cu^{III}(NH_3)_x^{3+}$, $Cu^{III}(en)_x^{3+}$ (en = ethylenediamine), and $Cu^{III}G_x^{(2-x)+}$, generated by pulse radiolysis techniques,[16] have an intense, broad absorption at ~300 nm. The transient copper(III) dimer, $Cu^{III}_2(O)(OH)_7^{3-}$, has equal-intensity absorption bands at 270 and 362 nm with $\epsilon \cong 9500$ M^{-1} cm^{-1} per Cu(III).[17] The electronic spectra of copper(III) complexes of macrocyclic ligands with amine and imine nitrogen donor atoms have several charge-transfer transitions in the 40 000–25 000-cm^{-1} (250–500-nm) region.[18] However, for the copper(III)–peptide complexes, we believe the chromophore structure is the copper(III)–N(peptide) unit (**5**) rather than copper(III)–N(amine) or copper(III)–O-

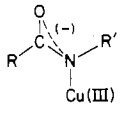

5

(carboxylate) because the two-band LMCT spectrum is seen for copper(III)–peptide complexes that have only N(peptide) donor atoms, such as $Cu^{III}(H_{-4}C)^{-6}$ (**6**) and copper (III)

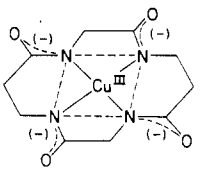

6

N-formyl peptides,[10] $Cu^{III}(H_{-4}$-*N*-$fG_4)^{2-}$ (**7a**) and Cu^{III}-$(H_{-4}$-*N*-$fG_3a)^-$ (**7b**). The chromophore unit (**5**) has both σ-

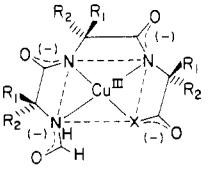

7a, $R_1 = R_2 = H$, $X = NCH_2CO_2^-$
b, $R_1 = R_2 = H$, X = NH

and π-symmetry molecular orbitals relative to the copper(III)–N(peptide) bond. The assignment of the low-energy band in the copper(III)–peptide spectra as π N(peptide)-to-copper(III) charge transfer and high-energy band as σ N(peptide)-to-copper(III) charge transfer is consistent with that given for the two LMCT bands in the electronic spectra of other d^8 transition-metal–halide complexes.[9,19,20] If LMCT

(16) Meyerstein, D. *Inorg. Chem.* **1971**, *10*, 2244.
(17) Gray, E. T., Jr.; Taylor, R. W.; Margerum, D. W. *Inorg. Chem.* **1977**, *16*, 3047.
(18) Olson, D. C.; Vasilevskis, J. *Inorg. Chem.* **1971**, *10*, 463.
(19) Gray, H. B.; Ballhausen, C. J. *J. Am. Chem. Soc.* **1963**, *85*, 260.

transitions from O(carboxylate) or N(amine) exist, their energy must overlap with that from N(peptide). A comparison of the spectra of copper(III) complexes with two to four deprotonated peptide nitrogens, with zero to one amine groups, and with zero to one carboxylate groups indicates that the absorption intensity is largely due to N(peptide)–Cu(III) LMCT transitions. The replacement of an N(peptide) group by a carboxylate group causes a 25% decrease in the intensity of the π-LMCT band. Also the σ-LMCT band is much broader for the tetrapeptide complexes than for the tripeptide amide or tripeptide complexes. For **6** the high-energy LMCT band is split into two high-intensity bands. The symmetry of **6**, C_{2h}, permits both the σ-LMCT and π-LMCT transitions to be split into two allowed transitions. Splitting of the σ-LMCT band for $Cu^{II}(asym\text{-}R_2en)_2^{2+}$, which has C_{2h} symmetry, compared to that of $Cu^{II}(sym\text{-}R_2en)_2^{2+}$ has been observed previously.[21] Although the copper(III) tetrapeptide and tripeptide amide complexes have lower symmetry, only one σ-LMCT band and one π-LMCT band are observed.

Another noteworthy trend is the red shift for both the σ- and π-LMCT bands as the number of α-carbon methyl groups in the ligand backbone increases. The red shift is much greater for the σ-LMCT transition (1500–2300 cm^{-1}) than for the π-LMCT transition (600–700 cm^{-1}). The inductive effect of the α-carbon methyl groups apparently increases the energy of the σ more than the π molecular orbitals (mainly nitrogen p_z), which is in accord with the transmission of electron density through the σ-bond framework. Apparently, the level of the metal-localized $d_{x^2-y^2}$ antibonding orbital is not significantly affected by α-carbon methyl group substitution. This is noted by the invariance of the maximum for the envelope of LF transitions for the tetrapeptides ($\sim$550 nm) and by the different effect α-carbon methyl group substitution has on the σ-and π-LMCT maxima. In contrast, a significant blue shift ($\sim$2000 cm^{-1}) for σ- and π-LMCT maxima is seen upon increasing the number of N(peptide) donors to copper(III), i.e. tripeptides vs. tetrapeptides or tripeptide amides.

The effect of nonaqueous solvents on the LMCT transition maxima also supports the σ and π assignment. The energy of the σ-LMCT band is essentially unaffected by changes in solvent whereas the energy of the π-LMCT band decreases in the order H_2O > 2-propanol > pyridine $\simeq$ CH_3CN, Me_2SO. Referring again to the ground-state chromophore structure **5**, solvents capable of hydrogen bonding to the excess electron density in the deprotonated peptide unit can stabilize the molecular orbital that has predominantly π character (nitrogen p_z) and lower its energy relative to the energy of the peptide nitrogen σ molecular orbital. Thus, solvents capable of hydrogen bonding cause a blue shift in the π-LMCT band and only slightly affect the position of the σ-LMCT band.

Copper(III) Disappearance Quantum Yields. Lack of Cu(III) Dependence. The quantum yield for loss of $Cu^{III}(H_{-2}Aib_3)$, ϕ, is independent of the concentration of copper(III) as reported in Table II. The ϕ^{405} value is not affected by changes in Cu(III) from $(0.02\text{–}1.0) \times 10^{-2}$ M.

Wavelength Dependence. For the specific conditions of 0.1 M acetate, pH 5.0, and μ = 0.1 M ($NaClO_4$), ϕ is plotted in Figure 1 with reference to the $Cu^{III}(H_{-2}Aib_3)$ absorption spectrum. A marked wavelength dependence is seen where ϕ varies from 0.030 to 0.37 for the wavelength range 546–250 nm. The decrease in ϕ above 420 nm is real since the quantum yield data were corrected for the fraction of light absorbed (eq 2) if less than optically opaque solutions were photolyzed. A two-plateau quantum yield spectrum also is seen for the copper(III) tripeptide complex $Cu^{III}(H_{-2}AAib_2)$ as shown in Figure 2 with ϕ^{405} = 0.17 and ϕ^{278} = 0.29. Preliminary results for $Cu^{III}(H_{-2}A_3)$ give still smaller quantum yields with ϕ^{366} = 0.09 and ϕ^{278} = 0.22.[22] The quantum yield spectrum for the tetrapeptide complex $Cu^{III}(H_{-3}G_2AibG)^-$ is presented in Figure 3 with reference to the $Cu^{III}(H_{-3}G_2AibG)^-$ absorption spectrum. For this copper(III) complex the LF envelope is separated from the π-LMCT band. The disappearance quantum yield is relatively constant throughout the π-LMCT band and only begins to decrease in the LF band. The rapid decrease in ϕ for **1** in the 420–550-nm region is probably due to photoredox-inactive LF transitions, which are masked by the charge-transfer transition. For $Cu^{III}(H_{-3}G_2AibG)^-$, the difference between σ and π photoredox activity is more pro-

Table II. Disappearance Quantum Yields for $Cu^{III}(H_{-2}Aib_3)$

λ, nm	ϕ[a]	10^3[Cu(III)], M[b]	conditions[c]
546	0.030	4.1	pH 5
546	0.028 ± 0.004	0.18–8.6	pH 5[d]
509	0.13	1.9–8.9	pH 5
468	0.21	1.7	pH 5
405	0.23	9.7	pH 5
405	0.23	4.2	pH 5
405	0.23	1.6	pH 5
405	0.23	0.89	pH 5
405	0.23	0.86	pH 5, O_2 satd
405	0.22	0.18–1.8	pH 1
405	0.21	0.18	pH 1, O_2 satd
405	0.24	1.7	pH 7
405	0.24	1.1	pH 5, μ = 1.0 M (NaCl)
405	0.24	1.1	pH 5, μ = 1.0 M ($NaClO_4$)
366	0.23	0.74–1.4	pH 5
366	0.23	0.97	pH 9
366	0.22	1.1	90% 2-propanol, air satd
334	0.25	0.74–1.2	pH 5
302	0.30	0.74–1.2	pH 5
278	0.34	0.39–0.50	pH 5
278	0.33	0.39–0.50	pH 5, O_2 satd
278	0.28	0.50	pH 9
278	0.30	0.52	pH 1
250	0.37	1.0	pH 5

[a] Units mol einstein^{-1}. Precision is 2–5% unless noted. [b] Initial $Cu^{III}(H_{-2}Aib_3)$ concentration. [c] pH 1: 0.1 M $HClO_4$, pH 1.0. pH 5: 0.1 M acetate, pH 5.0, μ = 0.1 M ($NaClO_4$). pH 7: 0.043 M phosphate, pH 7.2. pH 9: 0.1 M carbonate, pH 9.0, μ = 1.0 M ($NaClO_4$). [d] 0.05 M acetate, pH 5.0, μ = 0.1 M ($NaClO_4$).

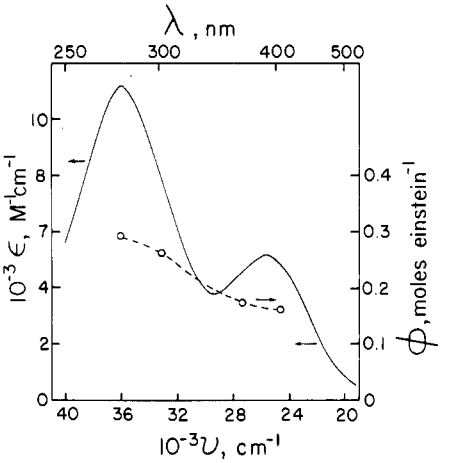

Figure 2. Disappearance quantum yield wavelength dependence and ultraviolet–visible absorption spectrum for $Cu^{III}(H_{-2}AAib_2)$ (0.1 M acetate, pH 5.0; μ = 0.1 M ($NaClO_4$)): ϕ, ---; UV–vis spectrum, —.

(20) Mason, W. R., III; Gray, H. B. *Inorg. Chem.* **1968**, *7*, 55.
(21) Kennedy, B. P.; Lever, A. B. P. *J. Am. Chem. Soc.* **1973**, *95*, 6907.
(22) Crawford, V.; Margerum, D. W., unpublished results.

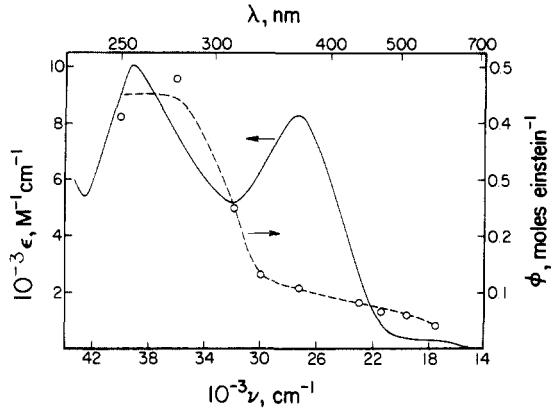

Figure 3. Disappearance quantum yield wavelength dependence and ultraviolet–visible absorption spectrum for $Cu^{III}(H_{-3}G_2AibG)^-$ (0.1 M acetate, pH 5.0, μ = 0.1 M ($NaClO_4$)): ϕ, ---; UV–vis spectrum, —.

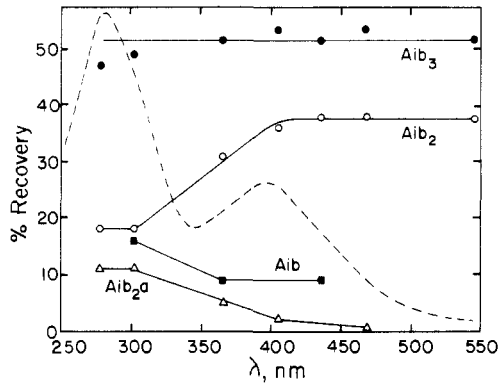

Figure 4. Photodecomposition stoichiometry (—) for $Cu^{III}(H_{-2}Aib_3)$ vs. the wavelength of irradiation with reference to the ultraviolet–visible absorption spectrum (---). The percent recovery is based on the [Cu(III)] lost (0.1 M acetate, pH 5.0, μ = 0.1 M ($NaClO_4$)).

nounced ($\phi(\sigma)/\phi(\pi) \approx 4$) than for the tripeptide–copper(III) complexes ($\phi(\sigma)/\phi(\pi) \approx 1.5$–2.4). To summarize, the two-plateau quantum yield spectrum appears to be characteristic of the photoactivity of copper(III)–peptide complexes. The presence of plateau regions within each LMCT band suggests that a different excited state with a characteristic reactivity toward redox decomposition is populated for irradiation of each LMCT band.

Medium Dependence. The wavelengths 278 nm for σ-LMCT photolysis and either 366 or 405 nm for π-LMCT photolysis were chosen to be representative of the dependence of ϕ on medium conditions for $Cu^{III}(H_{-2}Aib_3)$. As reported in Table II, ϕ^{405} or ϕ^{366} is independent of pH over the range 1–9; ϕ^{278} is only slightly dependent on solution pH. At pH 5 both ϕ^{278} and ϕ^{405} are unchanged when measured in O_2-saturated solution. Also, ϕ^{405} is unaffected by ionic strength changes from 0.1 to 1.0 M with use of NaCl or $NaClO_4$. Photolysis at 366 nm in 90% 2-propanol results in the same value of ϕ and qualitatively the same photodecomposition products as for photolysis of aqueous solutions.

Stoichiometry of Copper(III) Tripeptide Photodecomposition. Wavelength Dependence. The excited states produced by photon absorption in the LMCT spectral regions can be described as either σ or π copper(II)–amidyl radicals, σ-$Cu^{II}L\cdot{}^*$ or π-$Cu^{II}L\cdot{}^*$. The concept of π- and σ-radical primary photoproducts has been used to classify the photochemical reactions of organic compounds.[23] The $Cu^{II}L\cdot{}^*$ excited states can either emit, relax nonradiatively to ground state $Cu^{III}L$,

(23) Salem, L. *J. Am. Chem. Soc.* **1974**, *96*, 3486.

Table III. Wavelength Dependence of Photodecomposition Stoichiometry for $Cu^{III}(H_{-2}AAib_2)^a$

λ, nm	% recovery[b] Aib_2	AAiba	$AAib_2$
405	26 ± 1	3 ± 1	49 ± 2
366	22 ± 1	6 ± 1	48 ± 2
302	11 ± 1	11 ± 1	51 ± 2

[a] Complete photolysis of 1×10^{-3} M $Cu^{III}(H_{-2}AAib_2)$ in 0.1 M acetate, pH 5.0, μ = 0.1 M ($NaClO_4$). [b] Based on the amount of Cu(III) lost.

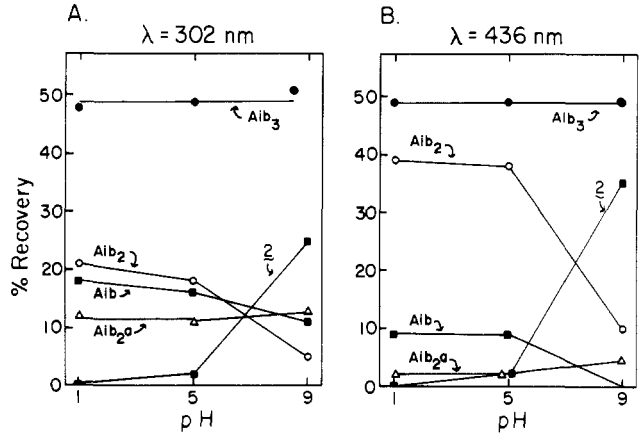

Figure 5. Photodecomposition stoichiometry for $Cu^{III}(H_{-2}Aib_3)$ vs. the solution pH. Irradiation wavelength: A, 302 nm; B, 436 nm. The percent recovery is based on the [Cu(III)] lost. Species **2** is a substituted hydantoin.

or react by pathways characteristic of the σ- and π-radicals (**8**–**11**). Emission from the copper(III)–tripeptide complexes

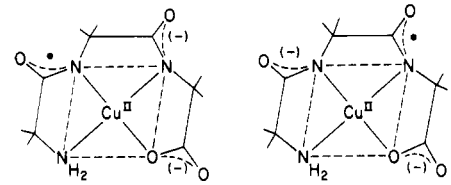

π-$Cu^{II}L\cdot{}^*$

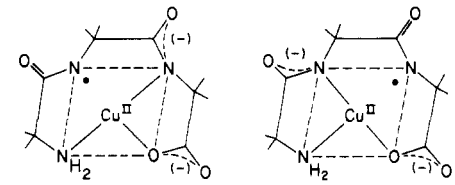

σ-$Cu^{II}L\cdot{}^*$

is not observed at room temperature in aqueous solution over the wavelength range 405–775 nm with excitation at 395 nm or from 290–660 nm with excitation at 280 nm. Thus, only decomposition competes with nonradiative decay of the excited state. For the photodecomposition of $Cu^{III}(H_{-2}Aib_3)$, the percent recoveries for the products of the tripeptide ligand photooxidation are plotted with reference to the $Cu^{III}(H_{-2}Aib_3)$ spectrum in Figure 4. The wavelength dependence of the photodecomposition stoichiometry for $Cu^{III}(H_{-2}AAib_2)$ is given in Table III. For both complexes the unchanged tripeptide is recovered in 50% yield independent of the wavelength of irradiation. Recovery of half of the original tripeptide suggests that the first one-electron oxidation of the ligand is caused by photoabsorption, but the second electron is lost via a thermal

Table IV. pH Dependence of Copper(III) Tripeptide Photodecomposition Stoichiometry

$Cu^{III}(H_{-2}Aib_3)$

λ, nm	pH	% recovery[a] Aib	Aiba	Aib_2	Aib_2a	Aib_3	2[b]
436	1[c]	9 ± 2	8 ± 1	39 ± 3	2 ± 1	49 ± 1	0
	5[d]	9 ± 2	<2[f]	38 ± 1	2 ± 1	49 ± 1	~2
	9[e]	<5[f]	<2[f]	10 ± 1	5 ± 1	49 ± 1	~31
302	1[c]	18 ± 2	16 ± 2	21 ± 1	12 ± 1	48 ± 2	0
	5[d]	16 ± 2	<2[f]	18 ± 1	11 ± 1	49 ± 1	~2
	9[e]	11 ± 2	<2[f]	5 ± 1	13 ± 1	51 ± 1	~22

$Cu^{III}(H_{-2}AAib_2)$

λ, nm	pH	% recovery[a] Aib	Aa	Aib_2	AAib	AAiba	$AAib_2$
436	1[c]	18 ± 2	15 ± 1	28 ± 1	0.5	2 ± 1	52 ± 2
	9[e]	g	g	6 ± 1	<0.3[f]	<4[f]	51 ± 2
302	1[c]	20 ± 2	22 ± 1	12 ± 1	1	12 ± 1	52 ± 2
	9[e]	g	g	2 ± 1	<0.3	12 ± 1	53 ± 2

[a] Based on the amount of Cu(III) lost for the complete photolysis of (0.1–1.0) × 10^{-2} M Cu(III). [b] Percentage estimated by the difference 100 − (% Aib + % Aib_2 + % Aib_2a + % Aib_3) at pH 9 and 436-nm irradiation. The other values for % 2 were then estimated from the relative peak heights in the RPLC chromatograms. [c] 0.1 M $HClO_4$. [d] 0.1 M acetate, pH 5, μ = 0.1 M ($NaClO_4$). [e] 0.1 M carbonate, pH 9, μ = 1.0 M ($NaClO_4$). [f] Limit of detection. [g] Not determined.

redox reaction of $Cu^{III}L$ with $Cu^{II}L\cdot$ (or with fragments from L·) to give L, L^+, and two copper(II) ions. The oxidized tripeptide, L^+, undergoes fragmentation and hydrolysis reactions to give the final products observed. The observed peptide fragments are dependent on the LMCT band irradiated as shown in Table III and Figure 4.

pH Dependence. From the data presented in Figure 4 wavelengths can be chosen that will be representative of the photooxidation products for irradiation of each LMCT band, i.e. 302 nm for σ-LMCT and 436 nm for π-LMCT. The change in photodecomposition product stoichiometry as solution pH is varied is presented in Figure 5 for $Cu^{III}(H_{-2}Aib_3)$. The pH dependence of the product stoichiometry for $Cu^{III}(H_{-2}AAib_2)$ photolysis is compared with that for $Cu^{III}(H_{-2}Aib_3)$ in Table IV. Except for the original tripeptide and the dipeptide amide yields, the stoichiometry and identity of the peptide products change as the pH of the copper(III) solution is varied from pH 1 and pH 9. This is informative because over the pH range 1–9 no change in the coordination of copper(III) occurs; however, the extent of coordination of copper(II) by the tripeptide ligand is a function of the solution pH. For $Cu^{II}Aib_3$, which has log K_1, pK_{a1}, and pK_{a2} values[24] of 5.11, 4.23, and 6.13, respectively, the Aib_3 complex would be completely dissociated at pH 1, partially dissociated at pH 5, and fully coordinated at pH 9 At pH 1 the copper(II)–Aib_3 complex dissociates with a rate constant $k_d \approx 10^6$ s^{-1}; [25] however, the radical species **8–11** would be expected to dissociate even faster than $Cu^{II}(H_{-2}Aib_3)$. Hence, at pH 1 $Cu^{II}L\cdot$ would rapidly dissociate to copper(II) and L· while at pH 9 $Cu^{II}L\cdot$ would be expected to undergo little or no dissociation. At pH 5 intermediate behavior and partial dissociation of L· from copper(II) would be expected during radical lifetime. Thus, product stoichiometry and identity depends on the extent of coordination of the amidyl radical by copper(II) during fragmentation of the radical ligand.

pH 1. For π-LMCT irradiation of $Cu^{III}(H_{-2}Aib_3)$ or $Cu^{III}(H_{-2}AAib_2)$, the major peptide fragments are dipeptide and amino acid, whereas for σ-LMCT irradiation the fragments are dipeptide, amino acid, and dipeptide amide. Fragmentation of an amidyl-radical tripeptide species by C–C bond cleavage, as shown by paths A, B, and C in Figure 6, accounts for the observed products. Previously, the small molecules carbon dioxide and acetone produced during π-LMCT photolysis were quantitated. The yields found were 53% and 47%,[3] respectively, based on the amount of copper(III) lost. Ammonia was estimated by the method of Forman[26] and was found to parallel the Aib_2 yields for all wavelengths; exact quantitation was difficult because all the other peptides, the amino acid, and the amino acid amide interfered with the assay. The fragmentation and redox reactions for $Cu^{II}L\cdot$ probably proceed through isocyanate intermediates, R—N=C=O, which hydrolyze to carbon dioxide and the Aib_2 or Aib products (eq 4–7 and 9).[27] Isocyanate formation via C–C bond cleavage is also observed for succinimidoyl radicals in a very rapid ring-opening process.[28] Likely intermediates for the amides are the (hydroxyalkyl)amides, $RCONHC(CH_3)_2OH$, which slowly hydrolyze to acetone and Aiba or Aib_2a (eq 7, 8, 10, and 11).[29] The dipeptide amide peak in the RPLC chromatograms of photodecomposed solutions increased with time reaching the maximum values reported in Table IV. Previously a triglycine alkylamide derivative, G_3NHCH_2OH, was isolated as a product of a decarboxylation reaction of the nickel(II)–G_4 complex.[30] The G_3NHCH_2OH derivative was observed to slowly decompose to G_3a and CH_2O.

$$Cu^{II}L\cdot \xrightarrow[Cu^{III}L]{\text{path A}} \underset{\mathbf{12}}{NH{=}C(CH_3)_2} + O{=}C{=}N\underset{\mathbf{13}}{C(CH_3)_2CONHC(CH_3)_2COOH} \quad (4)$$

$$\mathbf{12} \xrightarrow{H^+, H_2O} NH_4^+ + (CH_3)_2C{=}O \quad (5)$$

$$\mathbf{13} \xrightarrow{H_2O} CO_2 + Aib_2 \quad (6)$$

$$Cu^{II}L\cdot \xrightarrow[Cu^{III}L]{\text{path B}} \underset{\mathbf{14}}{NH_2C(CH_3)_2CONHC(CH_3)_2OH} + O{=}C{=}N\underset{\mathbf{15}}{C(CH_3)_2COOH} \quad (7)$$

$$\mathbf{14} \xrightarrow{H^+, H_2O} Aiba + (CH_3)_2C{=}O \quad (8)$$

$$\mathbf{15} \xrightarrow{H_2O} CO_2 + Aib \quad (9)$$

$$Cu^{II}L\cdot \xrightarrow[Cu^{III}L]{\text{path C}} \underset{\mathbf{16}}{NH_2C(CH_3)_2CONHC(CH_3)_2CONHC(CH_3)_2OH} + CO_2 \quad (10)$$

$$\mathbf{16} \xrightarrow{H^+, H_2O} Aib_2a + (CH_3)_2C{=}O \quad (11)$$

pH 9. The major peptide product from σ- and π-LMCT photodecomposition of the tripeptide copper(III) complex at pH 9 is the hydantoin **2**. Product **2** was the same for both $Cu^{III}(H_{-2}Aib_3)$ and $Cu^{III}(H_{-2}AAib_2)$ irradiations at pH 9 and was seen as the major oxidized tripeptide fragment for LMCT irradiation of $Ni^{III}(H_{-2}Aib_3)$ in 0.1 M $HClO_4$.[31] Figure 7 shows the copper(III)–tripeptide fragmentation pattern at pH 9 with σ-LMCT and with π-LMCT irradiation. Since no

(24) Hamburg, A. W.; Nemeth, M. T.; Margerum, D. W. *Inorg. Chem.* **1983**, *22*, 3535.
(25) Owens, G. D.; Margerum, D. W., unpublished results.
(26) Forman, D. L. *Clin. Chem. (Winston-Salem, N.C.)* **1964**, *10*, 497.
(27) Millar, I. T.; Springal, H. D. "Sidgwick's Organic Chemistry of Nitrogen", 3rd ed.; Clarendon Press: Oxford, 1966; p 463.
(28) Skell, P. S.; Day, J. C. *Acc. Chem. Res.* **1978**, *11*, 381.
(29) Challis, B. C.; Challis, J. In "The Chemistry of Amides"; Zalicky, J., Ed.; Wiley Interscience: New York, 1970; p 731.
(30) Bossu, F. P.; Paniago, E. B.; Margerum, D. W.; Kirksey, S. T., Jr.; Kurtz, J. L. *Inorg. Chem.* **1978**, *17*, 1034.
(31) Hamburg, A. W. Ph.D. Thesis, Purdue University, 1982.

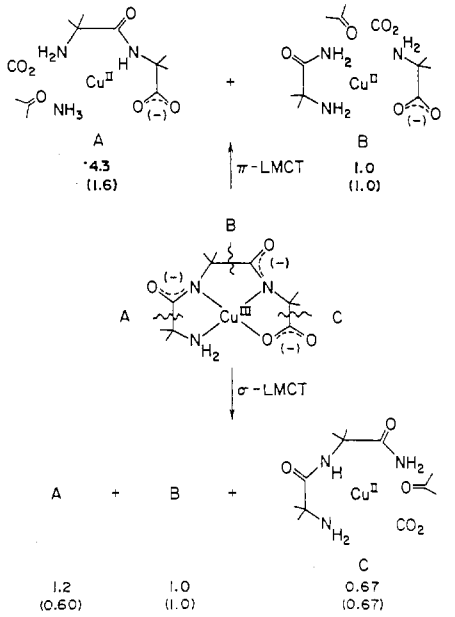

Figure 6. Fragmentation scheme for σ- and π-LMCT irradiation of copper(III)–tripeptide complexes at pH 1. Numbers under the capital letters are the relative yields for L = Aib_3 and for L = $AAib_2$ in parentheses.

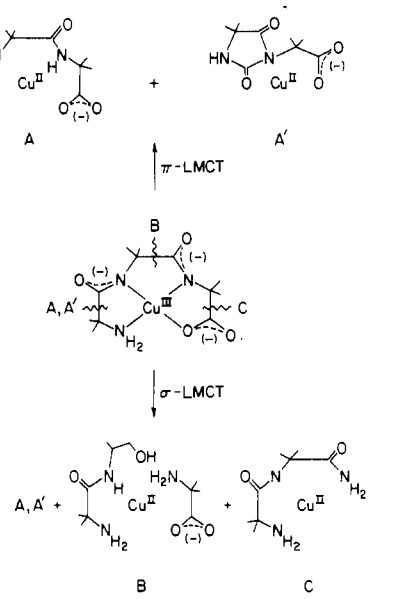

Figure 7. Fragmentation scheme for σ- and π-LMCT irradiation of copper(III)–tripeptide complexes at pH 9. The CO_2, NH_3 and $(CH_3)_2CO$ products are not shown.

amino acid amide is detected, a N-substituted amino acid amide, P1, is suggested to accompany Aib formation for path B fragmentation. (see the pH 5 discussion below.) Only peptide fragments are indicated since small molecules such as aldehyde or ketones, ammonia, or carbon dioxide were not assayed. Formation of the 3-substituted hydantoin **2** under mildly alkaline photolysis conditions probably occurs via intramolecular nucleophilic attack by the second deprotonated peptide nitrogen in the copper(II)-coordinated isocyanate intermediate (**17**) in eq 12. Hydantoins substituted in the

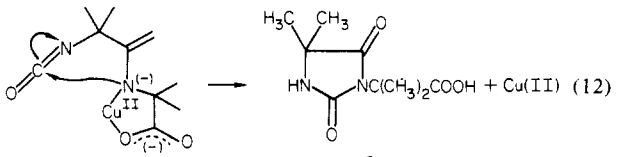

(12)

17 2

3-position are generally synthesized from the substituted isocyanate R′NCO and an amino acid[32] (eq 13), where the amino

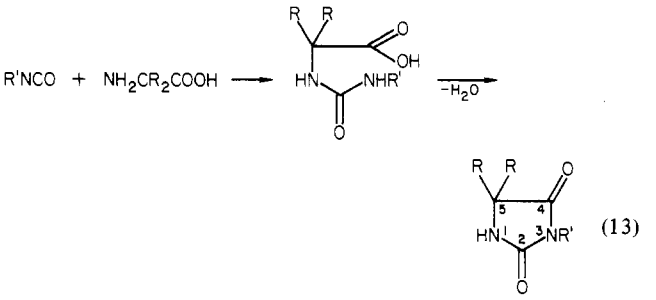

(13)

nitrogen is the nucleophile. Only at pH values where the peptide nitrogen in the isocyanate intermediate is coordinated to copper(II) (pH 9 and to a minor extent at pH 5) is the intramolecular reaction possible. Since **2** is also seen in the σ- and π-LMCT photodecomposition of $Ni^{III}(H_{-2}Aib_3)$ at pH 1,[31] neither the identity of the divalent metal in **17** nor the pH value of the photolysis solution is important. For photolysis of $Ni^{III}(H_{-2}Aib_3)$ at pH 1, the nickel(II)–ligand radical intermediates are expected to dissociate slowly since the dissociation reactions of nickel(II)–peptide complexes in acid solution are sluggish.[33]

pH 5. Table IV shows that product stoichiometry and identity at pH 5 is intermediate between that at pH 1 and pH 9. Instead of Aiba accompanying Aib production (path B, pH 1, Figure 6) a minor product, P1, with retention time between those Aib of and Aib_2a was seen. A suggested structure for P1 is a secondary amide, AibNHR or ANHR, where R may be $C(CH_3)=CH_2$ or $CH(CH_3)CH_2OH$. The retention time on the Altex C18 column for fragment P1 differs for $Cu^{III}(H_{-2}AAib_2)$ and $Cu^{III}(H_{-2}Aib_3)$ in accord with the presence of A or Aib in the first residue. The RPLC behavior of P1 supports the contention that P1 accompanies Aib formation in path B (Figure 7). The P1 product was not observed in the RPLC chromatograms of pH 9 photolysis mixtures because the analysis of the pH 9 photolysis mixtures was done on the Waters Radial-PAK C18 cartridge, which was less efficient than the Altex C18 column. The P1 product could not be detected on the Waters column in either pH 5 or pH 9 photolysis mixtures. The suggestion that P1 accompanies Aib formation at pH 9 (path B, Figure 7) is based on the pH 5 data on the Altex column and on mass balance considerations.

$Cu^{II}(H_{-2}Aib_3)$ Photodecomposition. At pH 9 any copper(II) present from the photodecomposition of $Cu^{III}(H_{-2}Aib_3)$ will be complexed by Aib_3 and the peptide fragments in solution. To determine if **2** could arise from the photodecomposition of the copper(II) complex, 5×10^{-3} M $Cu^{II}(H_{-2}Aib_3)^-$ in 0.1 M carbonate, at pH 9 and μ = 1.0 M ($NaClO_4$), was photolyzed at 302 and 436 nm. At 436 nm (irradiation of the copper(II) ligand field band, ϵ_{436} = 45 M^{-1} cm^{-1}) neither loss of tripeptide ligand nor change in absorbance of the copper(II) solution was seen; however, at 302 nm (irradiation of the low-energy side of a charge-transfer band, ϵ_{302} = 370 M^{-1} cm^{-1}) $Cu^{II}(H_{-2}Aib_3)^-$ is lost with a quantum yield of 0.02. The product of the 302-nm photolysis is **2**. The quantum yield for production of **2** from $Cu^{II}(H_{-2}Aib_3)^-$ is too low to account for the large amounts of **2** formed from the photolysis of $Cu^{III}(H_{-2}Aib_3)$ at pH 9.

Detection of Ligand Radical Species. No paramagnetic species were detected in the spin-trap experiments except for the copper(II) resonances. Although PBN and DMPO do not react with copper(III), any adduct formed between the nitrones and ligand radicals will still be radical species and could be

(32) Wade, E. *Chem. Rev.* **1950**, *46*, 403.
(33) Kennedy, W. R.; Margerum, D. W., to be submitted for publication.

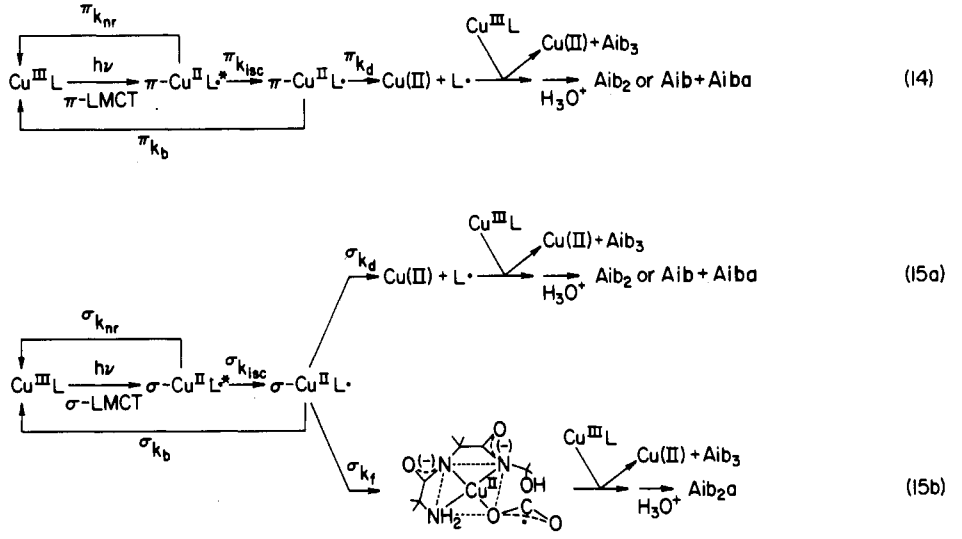

Figure 8. Mechanism for the photodecomposition of copper(III)–tripeptide complexes at pH 1.

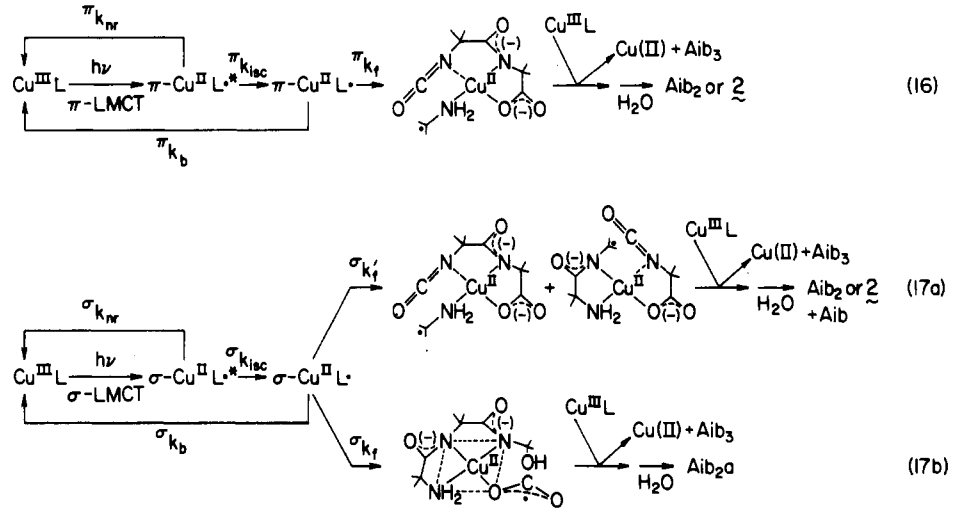

Figure 9. Mechanism for the photodecomposition of copper(III)–tripeptide complexes at pH 9.

oxidized by copper(III). Thus, the negative results from the spin-trap experiments do not eliminate a radical primary photoproduct. A $Cu^{II}L\cdot$ primary photoproduct is favored over a $Cu^{I}L^{+}$ species since the latter would be a very high-energy primary photoproduct.[23] However, copper(I) pathways may exist in the thermal decomposition of $Cu^{II}L\cdot$ since copper(II) is known to react rapidly with various carbon- and oxygen-centered radicals to give copper(I).[34]

Mechanism of Copper(III) Tripeptide Photodecomposition. A mechanism for the photodecomposition of copper(III)–tripeptide complexes must explain (1) the absence of a $Cu^{III}L$ concentration effect on ϕ (Table II), (2) the different products for σ- and π-LMCT photolysis (Table IV), (3) a pH dependence for the yield of dipeptide, amino acid, and hydantoin, but no pH dependence for the yield of dipeptide amide or tripeptide (Figure 5), and (4) a higher photodegradation efficiency for σ-LMCT band irradiation than for π-LMCT band irradiation (Figures 1–3). A mechanism that satisfies these requirements for the photodecomposition of copper(III)–tripeptide complexes at pH 1 is given by eq 14 and 15 in Figure 8. The rate constants k_{nr}, k_{isc}, and k_b designate, respectively, nonradiative decay of the initially formed singlet excited state, $Cu^{II}L\cdot{}^{*}$, intersystem crossing to a triplet state, $Cu^{II}L\cdot$, and electron back-transfer from the triplet state to give $Cu^{III}L$. The rate constants k_d and k_f refer, respectively, to L· dissociation from copper and L·fragmentation while it is coordinated to copper(II). Reaction of the second $Cu^{III}L$ molecule with the peptide radical after the irreversible dissociation of $Cu^{II}L\cdot$ (k_d, eq 14 and 15a) or after C–C bond cleavage (eq 15b) precludes a dependence of ϕ on the concentration of $Cu^{III}L$. (An alternative explanation for the lack of a concentration dependence in $Cu^{III}L$ is that the electron back-transfer pathways, ${}^{\pi}k_b$ and ${}^{\sigma}k_b$, do not exist, but this is unlikely.) A similar description of the photodecomposition reaction at pH 9 is given by eq 16 and 17 in Figure 9. In this case dissociation of $Cu^{II}L\cdot$ is expected to be much slower than fragmentation of L·.

The constancy of the dipeptide amide recovery over the pH range 1–9 for σ- and π-LMCT irradiation compared to changes in Aib_2, Aib, and **2** recoveries suggests that the formation of the dipeptide amide occurs before the steps that distinguish the pH 1 mechanism from the pH 9 mechanism, i.e. 15b in Figure 8 and eq 17b in Figure 9. The dipeptide amide is always a minor product for π-LMCT irradiations regardless of the solution pH value, whereas the σ states give major amounts of the dipeptide amide. The low yield of the dipeptide amide from π-$Cu^{II}L\cdot$ is due to a symmetry restriction, i.e. poor overlap of the incipient σ radical (from C–C bond cleavage) with the π nitrogen radical in **9**.[28,35] That is, the incipient σ radical from C–C bond cleavage in the third amino

(34) Ferraudi, G.; Muralidharan, S. *Coord. Chem. Rev.* **1981**, *36*, 45.

(35) Koenig, T.; Wielesek, A. *Tetrahedron Lett.* **1975**, 2007.

Table V. Quantum Yield Dependence on the Number of α-Carbon Methyl Groups[a]

peptide	R_1[b]	R_2[b]	R_3[b]	R_4[b]	$\phi(\sigma)$	$\phi(\pi)$	$\phi(\sigma)/\phi(\pi)$
Aib_3	Me, Me	Me, Me	Me, Me		0.34	0.23	1.5
$AAib_2$	Me, H	Me, Me	Me, Me		0.29	0.17	1.7
A_3[c]	Me, H	Me, H	Me, H		0.22	0.09	2.4
Aib_3a[d]	Me, Me	Me, Me	Me, Me		0.37	0.17	2.2
Aib_3G[e]	Me, Me	Me, Me	Me, Me	H, H	0.42	0.21	2.0
G_2AibG	H, H	H, H	Me, Me	H, H	0.45	0.11	4.1
G_4	H, H	H, H	H, H	H, H		0.06	
C[f]	g	H, H	g	H, H	0.008		

[a] Me is CH_3. [b] Refers to structure 18. [c] Reference 22. [d] Hinton, J. P.; Margerum, D. W., unpublished results. [e] Axup, A.; Hinton, J. P.; Margerum, D. W., unpublished results. [f] Reference 6. [g] β-alanyl residue; see structure 6.

acid residue of **9** would be oriented in a plane perpendicular to that of the π nitrogen radical. This would produce a high-energy diradical intermediate. In contrast, a similar fragmentation of the σ-$Cu^{II}L\cdot$ species would lead to overlap with the σ-nitrogen radical. The symmetry restriction for fragmentation of π-L· to give the observed products would be unimportant in the dissociated L· for two reasons. First, although the π configuration is generally accepted as the ground state of an amidyl radical system,[28,35] an EPR spectroscopic study has shown that bulky *N*-alkyl groups such as the *tert*-butyl group cause the R′CO and CNR planes to be twisted.[36] The bulkiness of the α-carbon methyl groups in the Aib unit fit into this category. Thus, the requirements of strict orthogonality of the π radical and the incipient σ radical from C–C bond fragmentation in uncomplexed L· would be relaxed. Second, the uncomplexed π-L· species may react with a second $Cu^{III}L$ before fragmentation, and radical species may not be involved in the fragmentation.

The high Aib_2/Aib ratio for π-LMCT irradiation of $Cu^{III}(H_{-2}Aib_3)$ at pH 1 (4.3 compared to 1.2 for σ-LMCT irradiation, Figure 6) requires **8**, the first-peptide-nitrogen radical, to be the major contributing species to π-$Cu^{II}L\cdot$. That is, the π-$Cu^{II}L\cdot$ photoproduct **8** must be at lower energy relative to **9** so that the former is preferentially populated by π-LMCT radiation. After dissociation of **8**, the first-peptide-nitrogen radical fragments predominantly along path A in Figure 6 because the formation of the tertiary radical species $NH_2\dot{C}(CH_3)_2$ is preferred over formation of the acyl radical from path B. For σ-LMCT irradiation, fragmentation of the ligand radical is less specific implying that dissociation of L· from copper(II) occurs before equilibration between **10** and **11**. Since for the σ-$Cu^{II}L\cdot$ species, **10** and **11**, some degree of bonding breaking already exists, ${}^{\sigma}k_d > {}^{\pi}k_d$ is expected. That is, dissociation of σ-$Cu^{II}L\cdot$ gives a similar distribution of the first- and second-peptide-nitrogen amidyl radicals that fragment by C–C bond cleavage along paths A, B, and C with less preference for a particular path.

A high Aib_2/Aib ratio could also be interpreted in terms of a copper(II)–N(amine) radical rather than a copper(II)–N(peptide) radical precursor. The copper(II)–N(amine) radical could only give Aib_2 by C–C cleavage in the first Aib residue (path A). However, a copper(III)–N(amine) charge-transfer state is expected to occur at higher energy than the copper(III)–N(peptide) state since the depronated peptide nitrogen should be more easily oxidized than amine nitrogen. Thus, the high Aib_2/Aib ratio for π-LMCT irradiation at pH 1 is attributed to the preferential population of **8** vs. **9** with selective fragmentation at path A after dissociation.

The higher quantum yield for σ-LMCT irradiation vs. π-LMCT irradiation suggests ${}^{\sigma}k_d > {}^{\pi}k_d$, which is plausible since in **10** and **11** there already exists a degree of Cu^{II}–N bond breaking as mentioned above. Also, the k_f pathway (eq 15b in Figure 8 and eq 17b in Figure 9 to form a dipeptide amide) provides an additional decay path for σ-$Cu^{II}L\cdot$ that is not available for π-$Cu^{II}L\cdot$.

Effect of Peptide Structure on φ. Table V presents φ as a function of the number of hydrogens bonded to the α-carbon in the copper(III)–peptide complex (**18**). A general decrease

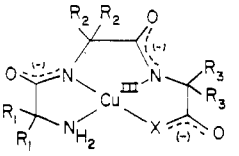

18

X = O, tripeptide
X = NH, tripeptide amide
X = $NC(R_4)_2CO_2^-$, tetrapeptide

is seen for both $\phi(\sigma)$ and $\phi(\pi)$ as the number of hydrogens bonded to the peptide backbone α-carbon is increased. For the tripeptides, the decrease in φ is more important for $\phi(\pi)$ than for $\phi(\sigma)$ as seen by the increasing ratio $\phi(\sigma)/\phi(\pi)$ with increasing numbers of α-carbon hydrogens. This decrease in φ suggests that α-C–H vibration promotes the nonradiative relaxation of the excited state,[37] i.e. k_{nr} is increased relative to k_d and k_{isc} or k_f and k_{isc} in eq 14–17. The rate constants ${}^{\sigma}k_d$ and ${}^{\sigma}k_f$ are thought to be larger than ${}^{\pi}k_d$ and ${}^{\pi}k_f$ because the σ ligand radicals formed from σ-LMCT irradiation should be more reactive toward fragmentation (no stabilization by delocalization is possible). Hence, the effect on φ for a given increase in k_{nr} will be more pronounced for the system with the smaller k_d (or k_f). This same effect is seen in the tetrapeptide and tripeptide amide φ values. There is little difference in $\phi(\sigma)$ for Aib_3a, Aib_3G, and G_2AibG whereas $\phi(\pi)$ is dependent upon ligand structure and is lower for the peptide with more α-carbon hydrogens. Thus, the effect of ligand structural variations on φ is greater for the less reactive π-$Cu^{II}L\cdot$ excited states. However, the two-plateau φ spectrum is general for the copper(III)–peptide complexes, which suggests that both σ- and π-excited states are populated and have different reactivities toward redox decomposition.

Effect of Tripeptide Structure on the Stoichiometry of Photodecomposition Products. At pH 1 the Aib_2/Aib product ratio is much lower for $Cu^{III}(H_{-2}AAib_2)$ than for $Cu^{III}(H_{-2}Aib_3)$ for both σ- and π-LMCT irradiation. The difference in structure is that $AAib_2$ has one α-carbon hydrogen in the first residue. The lower Aib_2/Aib ratio is accounted for by the same C–H vibronic relaxation effect seen for the disappearance quantum yields. Irradiation of the π-LMCT band produces both π-$Cu^{II}L\cdot$ radicals, **8** and **9**; however, **8** for $Cu^{III}(H_{-2}AAib_2)$ is depleted relative to **8** for $Cu^{III}(H_{-2}Aib_3)$ because of C–H vibrational relaxation. An additional factor possibly contributing to the lower Aib_2/Aib ratio for $Cu^{III}(H_{-2}AAib_2)$ is that fragmentation via path A would generate the less stable and unfavorable secondary radical NH_2CHCH_3.

(36) Sutcliffe, R.; Griller, D.; Lessard, J.; Ingold, K. U. *J. Am. Chem. Soc.* **1981**, *103*, 624.

(37) Streb, W.; Ballhausen, C. *Mol. Phys.* **1978**, *36*, 1321.

Similar fragmentation for $Cu^{III}(H_{-2}Aib_3)$ gives the tertiary radical $NH_2\dot{C}(CH_3)_2$. Thus, the presence of the α-carbon hydrogen in the first peptide residue increases the favorability of carbon–carbon cleavage by paths B and C over path A. The dipeptide amide yield for σ- and π-LMCT irradiation is the same for both $Cu^{III}(H_{-2}AAib_2)$ and $Cu^{III}(H_{-2}Aib_3)$. This supports the argument that the dipeptide amide is formed from a prompt cleavage of the $Cu^{II}L^{\cdot}$ state (eq 15b and 17b (path C)). Since the two tripeptides are identical at the carboxylate end, similar dipeptide amide yields are seen.

Conclusions

The ultraviolet–visible absorption spectra for copper(III)–peptide complexes show two ligand-to-metal charge-transfer bands. The assignment proposed for the bands is σ N(peptide)-to-copper(III) charge transfer for the 250–280 nm band and π N(peptide)-to-copper(III) charge transfer for the 360–400 nm band. The assignment is consistent with the photochemical behavior of copper(III)–peptide complexes as well as with the electronic spectral features of other d^8 transition-metal complexes of ligands with σ and π symmetries.

The photoredox decomposition of copper(III)–peptide complexes containing the α-aminoisobutyric acid residue is very efficient. The wavelength dependence of the disappearance quantum yield exhibits plateau regions for both the σ- and π-LMCT bands with $\phi(\sigma)$ varying from 0.008 to 0.45 and $\phi(\pi)$ varying from 0.09 to 0.23. The quantum yield spectrum depends on the length of the peptide ligand as well as the number of α-carbon methyl groups. The ϕ values decrease as hydrogen atoms are substituted for the methyl groups. It is suggested that an increased rate constant for nonradiative relaxation promoted by C–H vibrations is responsible for the decrease in ϕ.

The primary photoproducts proposed for the photodecomposition are σ and π copper(II)–amidyl radicals. For the tripeptide complexes both dissociation from copper(II) and fragmentation of the amidyl radicals are very rapid processes and occur before redox reactions with the copper(III) complex. The products of the photodecomposition of copper(III) tripeptides are copper(II) in 100% yield and the original tripeptide ligand in 50% yield (based on the initial amount of copper(III)) independent of the irradiation wavelength or solution pH. The remaining 50% of the tripeptide ligand is recovered as peptide fragments, acetone, carbon dioxide, and ammonia. The relative proportions and identity of peptide fragments depend on the LMCT band irradiated and on solution pH. In acid the copper(II)–amidyl radical dissociates into copper(II) and the amidyl radical. Initial fragmentation is by C–C bond cleavage followed by reduction of a second copper(III)–tripeptide complex and hydrolysis to give the amino acid, amino acid amide, dipeptide, and dipeptide amide. In base the divalent-metal-catalyzed formation of a 3-substituted hydantoin is the predominant reaction with smaller amounts of the peptide fragments seen in acid.

In summary, although the initially populated singlet LMCT excited state is probably very short-lived, another $Cu^{II}L^{\cdot}$ state (triplet probably), **8–11**, has a lifetime long enough for reactions that are dependent on medium conditions to occur such as dissociation of the $Cu^{II}L^{\cdot}$ species before fragmentation. When fragmentation of $Cu^{II}L^{\cdot}$ occurs, the reactivity is governed by the σ or π symmetry of the radical species.

Acknowledgment. This investigation was supported by Public Health Service Grant No. GM 19775 from the National Institute of General Medical Sciences, by a Phillips Petroleum Fellowship (A.W.H.), and by American Chemical Society Analtyical Division Summer Fellowship sponsored by the Society of Analytical Chemists of Pittsburgh (A.W.H.). The assistance of Professor David R. McMillin during this work is gratefully acknowledged.

Registry No. **1**, 69990-31-4; **2**, 87783-57-1; $Cu^{III}(H_{-2}AAib_2)$, 87801-41-0; Aib_3, 50348-89-5; $AAib_2$, 83917-78-6; Aib, 62-57-7; Aiba, 16252-90-7; Aib_2, 39692-70-1; Aib_2a, 87453-26-7; Aa, 7324-05-2; AAib, 84799-80-4; AAiba, 87453-25-6; $(CH_3)_2C{=}O$, 67-64-1; ammonia, 7664-41-7.

Contribution from the Department of Chemistry, University of Hong Kong, Hong Kong

Structural and Mechanistic Studies of Coordination Compounds. 36. Electronic Spectra and Photochemistry of Some *trans*-(Tetraamine)ruthenium(III) Complexes

CHUNG-KWONG POON,* TAI-CHU LAU, and CHI-MING CHE

Received June 7, 1982

The electronic absorption spectra of an extensive series of tetraamine complexes of the type *trans*-$[RuLX_2]^+$ (X = Cl, Br, or I) have been analyzed. In general, two ligand-to-metal charge-transfer (CTTM) transitions of $(p_\pi)_X \rightarrow d_\pi^*$ origin are observed. The wavelength of the lowest energy band increases gradually with increasing chelation and steric congestion of the amine ligand L around the ruthenium(III) ion. The splitting of the $(p_\pi)_X \rightarrow d_\pi^*$ transition is largest for the two sterically congested teta and tetb complexes, where teta and tetb represent *C-meso-* and *C-rac*-5,5,7,12,12,14-hexamethyl-1,4,8,11-tetraazacyclotetradecane, respectively, but decreases with the nature of X, Cl > Br > I. The spectra of *trans*-$[Ru(cyclam)X_2]X$ (X = Cl or Br) have been resolved at low temperature (~30 K), and $(p_\sigma)_X \rightarrow d_\pi^*$ transitions have been assigned to some of these resolved bands. Photochemistry of *trans*-$[RuLIX]^+$ (L = $(en)_2$, X = Cl, Br, or I; L = 2,3,2-tet or cyclam, X = I; en, 2,3,2-tet, and cyclam represent ethane-1,2-diamine, 3,7-diazanonane-1,9-diamine, and 1,4,8,11-tetraazacyclotetradecane, respectively) has been investigated. Irradiation at the lowest CTTM band (λ_{irr} > 500 nm) leads to stereoretentive aquation of X^- with quantum yields independent of X but decreasing with increasing chelation of L. Domination of the Ru^{II}–I· entity in the CTTM excited state has been discussed. Irradiation of the second CTTM band leads to photoaquation with concomitant stereochemical change. The results are interpreted in terms of a quartet ligand field state as the photoreactive precursor, and a dissociative model previously proposed to explain the photostereochemistry of d^6 metal complexes has been useful also for this d^5 system.

Introduction

The chemistry of ruthenium(III) amine complexes has been an area of active research in recent years.[1-4] However, relatively little photochemical work has been reported. It is generally believed that the low-lying and partially vacant d_π^*

(1) Ford, P. C. *Coord. Chem. Rev.* **1970**, *5*, 75.

(2) Taube, H. *Comments Inorg. Chem.* **1981**, *1*, 17.

(3) Broomhead, J. A.; Basolo, F.; Pearson, R. G. *Inorg. Chem.* **1964**, *3*, 826.

0020-1669/83/1322-3893$01.50/0